Heat and Mass Transfer (2020) 56:1365–1378
https://doi.org/10.1007/s00231-019-02795-8

ORIGINAL

Influence of moisture content on the thermophysical properties of tropical wood species

Rachel Raïssa Ngono Mvondo[1] · Jean Claude Damfeu[2] · Pierre Meukam[2] · Yves Jannot[3]

Received: 1 October 2018 / Accepted: 22 November 2019 / Published online: 10 December 2019

Abstract

The aim of this work was to investigate the thermal behavior of solid wood used as building materials. Three tropical wood species namely Iroko (*Milicia excelsa*), Bilinga (N*auclea diderrichii*), and Tali (*Erythrophleum suaveolens*) were chosen. The thermophysical properties in the longitudinal, radial and tangential directions were determined experimentally for different moisture contents. Asymmetrical hot plate method was used to measure the thermal conductivity and volumetric heat capacity. The influence of water content and the direction of the fibers on thermophysical properties of the species studied were investigated. The results show that thermal conductivity and volumetric heat capacity increase with moisture content, while the diffusivity decreases. In the wide range of moisture content considered, thermal conductivities varied between 0.1 and 0.6 Wm^{-1} K^{-1}. The increase of moisture content by 1% induces a 0.2% increase in thermal conductivity for Bilinga, 0.4% for Tali and 0.3% for Iroko. Tali, whose density is the highest, presented high values of thermal conductivity in longitudinal direction but lowest values in radial and tangential directions compared to other species. Thermal conductivity is 2 to 3 times higher in the longitudinal direction than in the radial and tangential directions. The volumetric heat capacity was not influenced by the direction of the heat flow.

Nomenclature

a	Thermal diffusivity of the sample (m^2 s^{-1})
c_p	Specific heat capacity of the sample (J kg^{-1} K^{-1})
c_{pdry}	Specific heat capacity of dried material (J kg^{-1} K^{-1})
c_{ph}	Specific heat capacity of the heating element (J kg^{-1} K^{-1})
c_{pi}	Specific heat capacity of the insulating material (J kg^{-1} K^{-1})
c_{pwater}	Specific heat capacity of water (J kg^{-1} K^{-1})
E	Thermal effusivity of the sample (J m^{-2} K^{-1} $s^{-1/2}$)
e_h	Thickness of the heating element (m)
e_i	Thickness of the insulating material (m)
E_i	Thermal effusivity of the insulating material (J m^{-2} K^{-1} $s^{-1/2}$)
e_s	Thickness of the sample (m)
m	Mass of the sample at time t (g)
m_0	Initial mass of the sample (g)
m_{dry}	Dry mass of the sample (g)
Rc	Thermal contact resistance (°C W^{-1})
RS	Reduced sensitivity (°C)
S	Heating element area (m^2)
t	Time (s)
T	Temperature (°C)
V	Volume (m^3)
X	Water content at time t (%)
X_0	Initial water content (%)

Greek letters

β	Coefficient used to estimate the volumetric heat capacity
δ	Coefficient used to determine the thermal effusivity
λ	Thermal conductivity (W m^{-1} K^{-1})
ρ	Apparent density (kg/m^3)
ρ_{dry}	Apparent density of dried material (kg/m^3)
ρ_{water}	Apparent density of water (kg/m^3)

Highlights - Thermal properties of wood species were measured using the asymmetrical transient hot plate method;
- Experimental results show that thermal conductivity is higher in the longitudinal direction than in the radial and tangential directions.
- Thermal conductivity increases considerably with increasing water content.

✉ Pierre Meukam
pierre_meukam@yahoo.fr

[1] University Institute of wood Technology, the University of Yaoundé I, P.O. Box 306, Mbalmayo, Cameroon

[2] Laboratory(L3E): Energy, Water and Environment, National Advanced School of Engineering, the University of Yaoundé I, P.O. Box 8390, Yaoundé, Cameroon

[3] LEMTA, Nancy-Université, CNRS, 2, Avenue de la Forêt de Haye, BP160, 54504 Vandoeuvre Cedex, France

ϕ_0 Heat flux in the heating element (W)
Ω Sum of quadratic errors

Abbreviations

comp Complete model
exp Experimental
mod Model
simpl Simplified model

1 Introduction

The objectives of the Kyoto Protocol were to reduce the global temperature by 2 °C by 2020 and to reach 1.5 °C by 2050 [1]. The increase in global temperature is linked to the increase in greenhouse gas (GHG) emissions. Several studies show that the building sector is the second largest sector producer of CO_2 after industry. CO_2 emissions in the building sector are mainly due to energy consumption [2, 3]. In France, for example, ADEME in its report on energy consumption in 2015 [4] revealed that 43% of CO_2 emissions came from the building sector. One of the solutions to reduce the rate of emission of CO_2 is to use renewable building materials. Among the buildings with these new types of building materials, those made of wood materials or with other materials incorporating wood fibers were identified. Indeed, the studies carried out by the Scientific and Technical Center of the Building (CSTB) [5] have shown that they are materials that require little energy for their transformation (low gray energy) and generally have low thermal conductivity. The second tropical timber reserve is in the Congo Basin in Africa. Cameroon in particular, has more than 2000 ha of forest. Field surveys have shown that nearly 98% of both residential and public buildings are constructed of sand-block materials ($\lambda = 1.17\ Wm^{-1}\ K^{-1}$ [6]). The high availability of timber should prompt Cameroon to further develop wooden constructions instead of sand blocks or laterite bricks which require higher cost and need more energy to provide thermal comfort of the occupants. Cameroon in particular has various species of wood. The challenge is to show that the use of wood as building material in place of other building materials can contribute in reducing energy consumption due to air conditioning. Thermal conductivity is the parameter which makes it possible to classify a material as an insulating material. Unlike other materials such as sand blocks or laterite bricks, wood is an anisotropic material with an internal structure that is distinguished from the others by fibers orientation in three directions. In a wood, the orientation of the fibers can influence the thermal conductivity. Several studies show that the thermophysical properties of wood differ according to the direction of sawing. Steinhagen [7] has shown that the orientation of molecular chains in the longitudinal direction leads to a higher thermal conductivity than in the tangential direction. Suleiman et al. [8] obtained the same value of thermal conductivity in the radial and tangential directions whereas other authors claim that transverse conductivity is higher in the radial than in the tangential direction [9–11]. Wood is also a hygroscopic material. The amount of water it contains can have a great influence on its thermophysical properties. Studies by Kol [12] showed that thermal conductivity in all three directions increased with moisture content (MC) between 0 and 22%. Sonderegger et al. [13] found a linear relationship between thermal conductivity and water content.

The presence of water strongly affects the heat capacity of wood because of the high heat capacity of water [14]. Ngohe-Ekam et al. [15] have carried out an experimental study on the thermal properties of five woods usually used in central Africa. The thermal properties were related to basal density and to MC using the box method. They presented experimental results between 0%–60% MC and 0.3–0.8 kg/m^3 of basal density. Results showed that conductivity and effusivity increase and thermal diffusivity decreases with increasing MC.

The objective of this work is to characterize Cameroonian timber species to justify their usage as construction materials with better thermal insulation performance than the materials presently used. For this purpose, the estimation of their thermophysical properties (thermal conductivity, volumetric heat capacity) in the three directions was the object of this work. The direction which gives a lower value of the thermal conductivity, taking into account the water content of the material, was determined. This information on timber from Cameroon should help architects in the choice of filling material for buildings. Most studies reported in the literature are focused on the characterization of wood for given moisture content. In the present research, the thermophysical properties of certain tropical wood species were investigated by the asymmetric hot plate method already used by many authors [16–18]. The effect of orientation of fibers on the thermophysical properties of some tropical wood species namely Iroko (*Milicia excelsa*), Bilinga (N*auclea diderrichii*), and Tali (*Erythrophleum suaveolens*), and how the water content affects these thermal properties was studied.

2 Material and sample preparation

2.1 Material

Wood species were cut in the southern Cameroonian forest. The choice was based on the most commercialized and commonly used species. Three selected species were Iroko (*Milicia excelsa*), Bilinga (N*auclea diderrichii*) and Tali (*Erythrophleum suaveolens*). Tali and Bilinga are high density woods while Iroko is a medium density wood. They are used in construction, carpentry, flooring and framing. Segments of wood were obtained from the heartwood region at green state and were cut from

successive portions of the same stem to obtain as many identical and uniform characteristics as possible. The physical and mechanical properties of the selected species were studied by Mvondo et al. [19]. The values obtained at 12% MC are presented in Table 1 [19].

The three tropical wood species have good durability with respect to the different types of fungi. Bilinga can be majority employed without preservation treatment and deforms little during drying. Iroko is not recommended in circumstances exposed to a permanent or prolonged humidification risk. It dries quickly and have no significant risk of cracking or deformation. Tali is recommended in all circumstances exposed to a risk of permanent humidification and tends to deform during drying [20].

2.2 Sample preparation

Firstly, the choice of samples used for the test was made according to the French standard NF B51–003 [19]. Then, sequences of 45 samples per species were selected. In a last step, 12 best samples per species were retained for the test. Four samples were manufactured for each direction.

- For each wood species, specimens were prepared by planning the board surfaces and sawing them into parallelepipeds with nominal dimension 100 mm × 100 mm × 10 mm (thick). The preparation was made in such a way that they permitted the measurement of the thermal conductivity along three orthogonal directions (LRT). For given water content, the mean value of measurements on three samples was retained.
- The samples were gradually dried in order to reduce their water content. To preserve from any undesirable gain or loss in moisture, all the treated specimens were stored in sealed plastic boxes until measurement.
- The samples were dried in an oven. After 6 weeks of measurement at different MC, as described by Siau [10], oven-dried samples were obtained using a drying temperature of 105 °C for a sufficient duration before a constant mass of the sample was obtained. After heating at such temperature, both the free and bound water in wood were released, and the specimens were completely dry. To obtain the mass of dried sample the electronic balance SF 400-A with a ± 0.01 g precision was used.

3 Determination of different parameters

3.1 Moisture content

From the dry mass obtained, the different water contents of the sample are deduced for each condition previously set. The water content in dry basis X is given by the mathematical expression [21]:

$$X = 100\left(\frac{m}{m_{dry}} - 1\right) = 100\left[\frac{m}{m_0}(1 + X_0) - 1\right] \quad (1)$$

where

X	is the water content of the sample at time t (%),
X_0	is the initial water content of the sample (%),
m	is the mass of the sample at time t,
m_0	is the initial mass of the sample,
m_{dry}	is the dry mass of the sample.

3.2 Apparent density

The water content and density are related by Eq. (2) [19].

$$\frac{\rho}{\rho_{dry}} = \frac{\rho_{water}(1 + X)}{\rho_{water} + X\rho_{dry}} \quad (2)$$

Where:

ρ_{water}	is the apparent density of water,
ρ_{dry}	is the apparent density of dried material.

Table 1 Physical and mechanical properties of selected species at 12% MC [19]

Wood species	Family	Apparent Density (kg/m^3)	Basal density (kg/m^3)	Maximum bending stress (MPa)	Young's modulus H = 12% (Mpa)	Applications
Iroko (*Miliciaexcelsa*)	Moraceae	550–750	0,64	87	10,300	Carpentry, framing, shipbuilding,
Bilinga ((N*aucleadiderrichii*)	Rubiaceae	730–890	0,65	95	11,800	Flooring, construction, vehicle floors, shipbuilding.
Tali (*Erythrophleumsuaveolens*)	Erythroxylaceae	800–1050	0,71	128	15,600	Heavy construction, bridges.

Table 2 Specific heat capacity of dried materials

T (°C)	20	30	40	50	60
Iroko (J kg^{-1} K^{-1})	1284	1327	1369	1415	1462
Tali (J kg^{-1} K^{-1})	1240	1276	1318	1360	1400
Bilinga (J kg^{-1} K^{-1})	1205	1245	1287	1326	1367

3.3 Measurement of thermal properties

3.3.1 Volumetric heat capacity

The specific heat capacity of dried material (c_{pdry}) was measured using Differential Scanning Calorimetry. To obtain the volumetric heat capacity (ρc_p) the dimensions of the samples were measured and their mass determined using the same balance for water content measurement. The relation allowed calculating the volumetric heat capacity according to the properties of the dried material and the water content can be expressed as:

$$\rho c_p = \rho_{dry}\left(c_{pdry} + X c_{pwater}\right) \tag{3}$$

Where c_{pwater} is the specific heat capacity of water.

$\rho c_p = f(X)$ is therefore a straight line. The measured values of c_{pdry} for selected species are given in Table 2.

3.3.2 Thermal conductivity

The thermal conductivity λ was calculated from measured values of thermal effusivity and volumetric heat capacity. The asymmetrical transient hot plate method was used. This method is presented by Bal et al. [17] and Damfeu et al. [21]. An experimental device designed with the sample was used in this study for measuring the thermal properties and is shown in Fig. 1.

For measuring thermophysical parameters, the sample was weighed and placed in an electric oven at 40 °C for 24 h. After 24 h, the sample was weighed again and packaged in the plastic bag for 1 week to obtain uniform water content throughout the sample and new thermal properties were then measured. This process was repeated at least five times for each sample before the sample was placed in the electric oven for 48 h at 105 °C. The mass of the dried sample was then measured. Four measures per wood direction were carried out for each selected species and the mean values were retained.

Several difficulties arise in determining thermal properties when the MC of the wood material is high. The effect of the moisture not only confounds the measurement but also raises some doubt about the practical significance of the results. When moist wood is subjected to a thermal gradient, a redistribution of the moisture takes place resulting in a transient heat flow. MacLean [22] observed that, in solid wood specimens of 0.5 to 0.75 mm in thickness with an initial MC below 12 to 15%, most of this redistribution generally took place

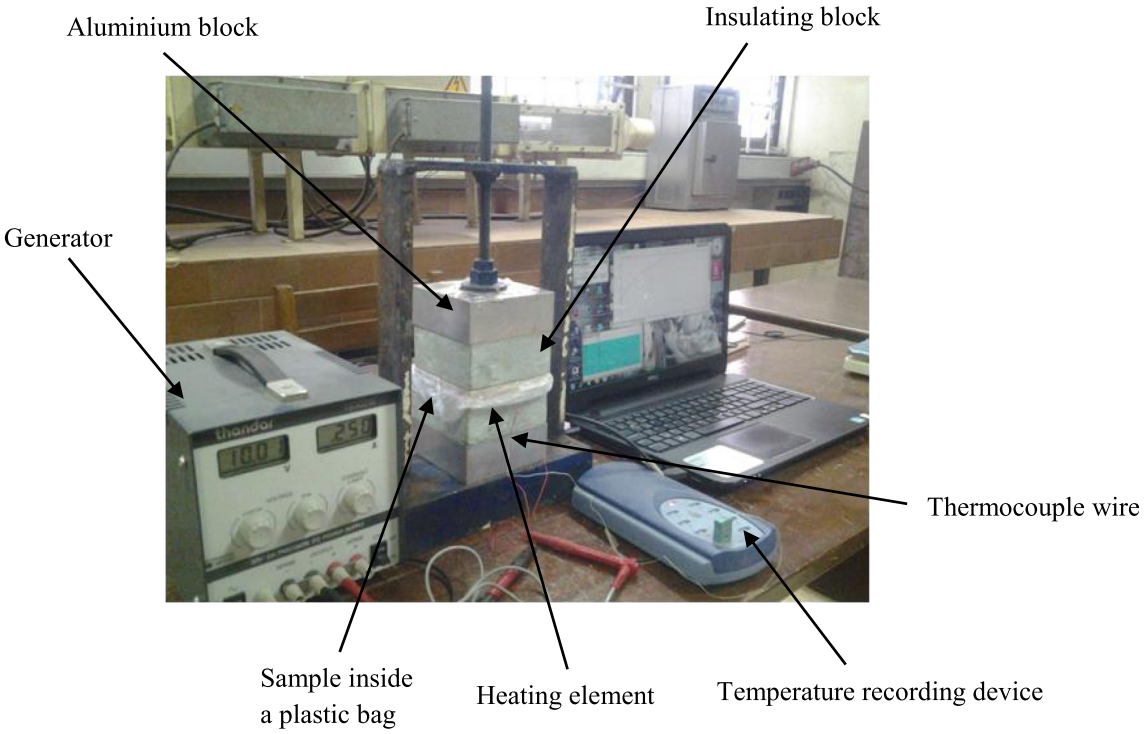

Fig. 1 Experimental device

within 24 h without significant change in conductivity after that. Usually equilibrium was reached after only 6 h.

4 Modelling

The simplified and complete models already developed by Bal et al. [17] and Damfeu et al. [21] can be used to determine thermal effusivity and volumetric heat capacity. The pre-estimated value of thermal effusivity was obtained from numerical calculation of the slope $\delta(t)$ of the linear part of the experimental curve $T(t) = f(\sqrt{t})$ as shown in Fig. 2b.

$$E = \frac{2\phi_0}{\delta\sqrt{\pi}} - E_i \tag{4}$$

Where:

E and E_i	are the thermal effusivities of the sample and insulating material ($Jm^{-2}K^{-1}s^{1/2}$).
ϕ_0	is the heat flux produced in the heating element (W).
δ	is a coefficient obtained numerically by calculating the slope of the linear part of the experimental thermogram $T(t) = f(\sqrt{t})$

It was also possible to evaluate the pre-estimated value of volumetric heat capacity. This may be approximated from the slope $\beta(t)$ of the linear part of the curve $T(t) = f(t)$ as shown in Fig. 2a. The calculation of this parameter is:

$$\rho c_p = \frac{1}{e_s}\left(\frac{\phi_o}{\beta} - \rho_i c_{pi} e_i - \rho_h c_{ph} e_h\right) \tag{5}$$

Where:

ρc_p, $\rho_i c_{pi}$ and $\rho_h c_{ph}$	are the volumetric heat capacities of the sample, the insulating material and the heating element respectively ($Jm^{-3}\ K^{-1}$).
e_s, e_i and e_h	are the thicknesses of the sample, the insulating material and the heating element respectively (m).
β	is a coefficient obtained numerically by calculating the slope of the linear part of the experimental thermogram $T(t) = f(t)$

5 The thermal properties estimation method

The asymmetrical hot plate method was used to measure the volumetric heat capacity and the thermal effusivity. The calibration process was already done by Damfeu et al. [21].

Thermal parameters of the insulating material were measured by center plate method and calculations were done with the values obtained by Jannot et al. [23, 24].

A complete model was used to estimate effusivity E and volumetric heat capacity ρc_p. The initial value used was the value pre-estimated from the simplified model with experimental temperatures.

The Levenberg Marquart algorithm integrated in the Matlab code was used to estimate the value of E and ρc_p which minimized the sum of quadratic errors $\Omega = \sum_{i=1}^{n} \left[\Delta T_{exp}(t_i) - T_{mod}(t_i)\right]^2$ [21] between the experimental data and theoretical data. The time interval $[t_0, t_{max}]$ was considered for the estimation such that residues are small and perfectly centered around 0 °C as shown in Fig. 3. This validates the 1D model. Damfeu et al. [21] noticed that above 15 °C,

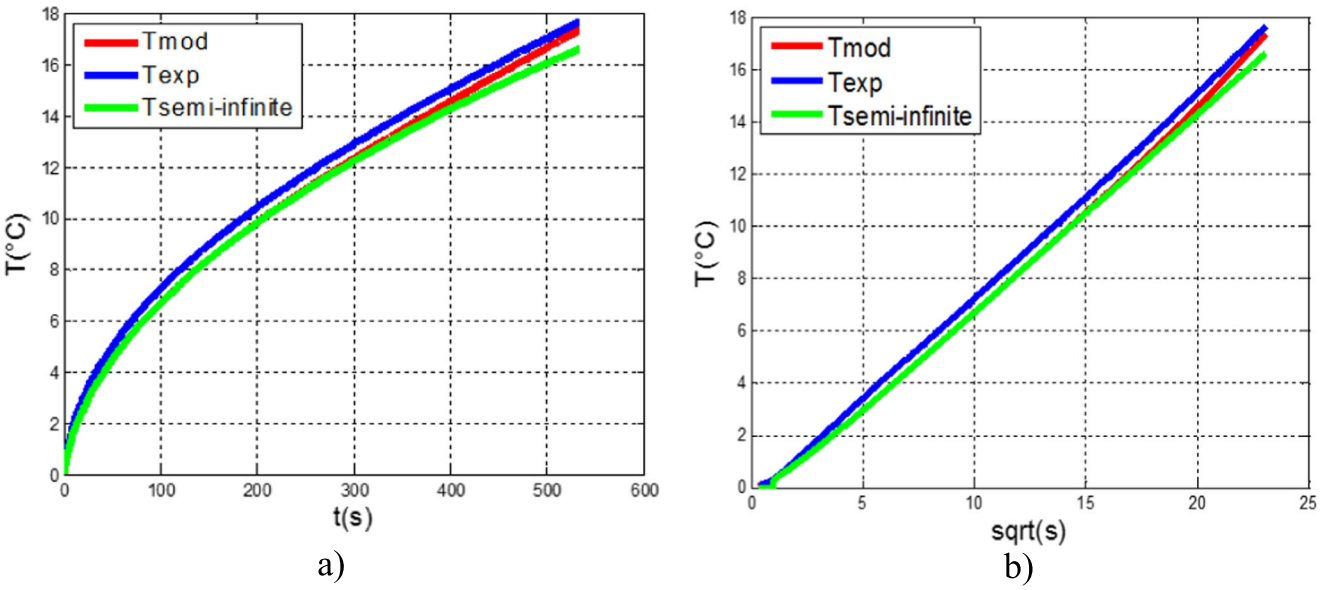

Fig. 2 Temperatures curves for Iroko a) $T = f(t)$, b) $T(t) = f(\sqrt{t})$

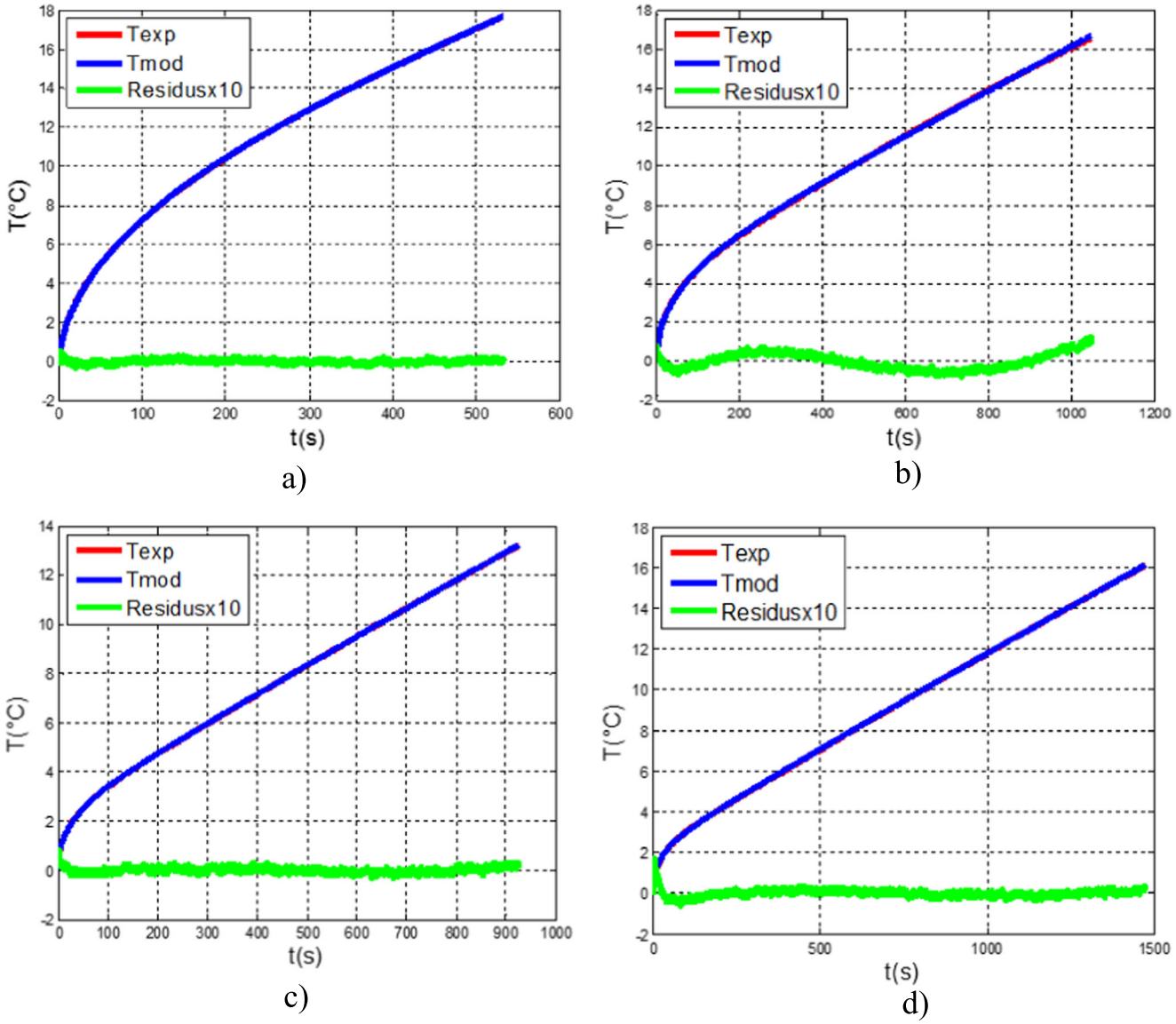

Fig. 3 Experimental and modeled curves with residues (×10) curves for: **a** Iroko at 7% MC, **b** Iroko at 32% MC, **c** Bilinga at 34%MC, **d** Tali at 35%MC

temperature variations can generate the 2D / 3D effects that characterize a bidirectional propagation of heat flux. The process being the same, we carried out the recordings up to 18 °C with estimation of the parameters over a time interval where the residues are centered around 0 °C. The results of uncertainty analysis were given in Table 3.

Table 3 Uncertainty analyses of the measurement

Uncertainties	Values
Thermal effusivity: the mean relative uncertainties estimated in form of standard deviation is	0,26%
Heating element thickness	±0,01 mm
Apparent density: average uncertainty of apparent density	0,67%
Specific heat capacity: the relative uncertainty on the measured value of Cp is estimated to:	2%

6 Sensitivity analysis

Sensitivity analysis is based on the interpretation of the reduced sensitivities of the temperature to a thermophysical parameter X [$X\frac{\partial T(t)}{\partial X}$]. The study of the reduced sensitivity curves then makes it possible to define the time intervals on which the best pre-estimation of thermal effusivity and volumetric heat capacity can be made.

– According to Fig. 4, the reduced sensitivities of the temperature to the thermal effusivity are uncorrelated to the other sensitivities between times 0 s and 200 s. This can allow a good pre-estimation of E in this time interval.

Fig. 4 Reduced sensitivity of the three species at 10% and 30% MC ▶ respectively: **a** Iroko, **b** Bilinga, **c** Tali

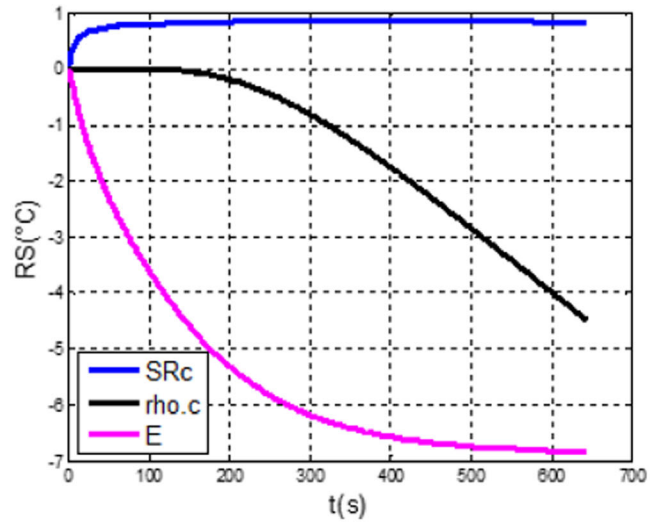
RS(°C)
t(s)
SRc
rho.c
E

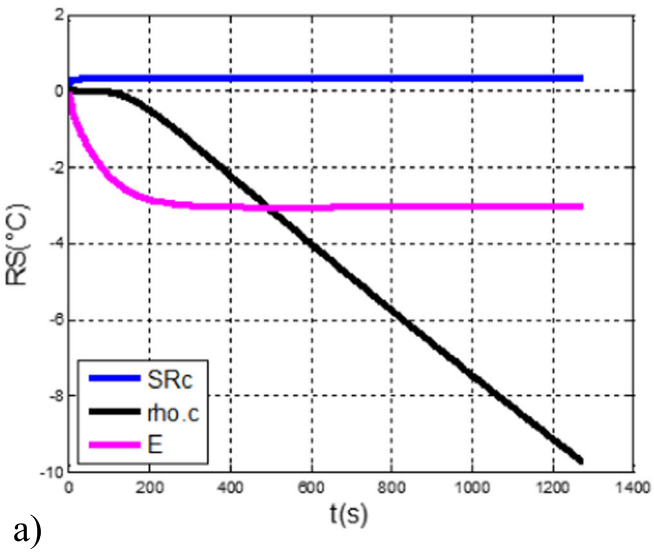
RS(°C)
t(s)
SRc
rho.c
E

a)

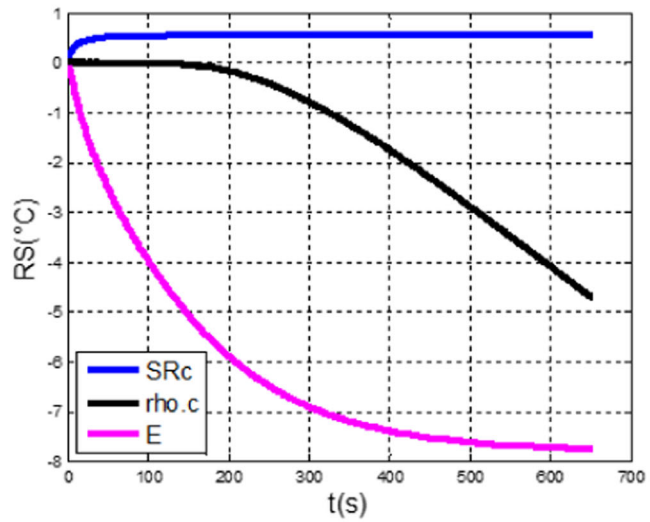
RS(°C)
t(s)
SRc
rho.c
E

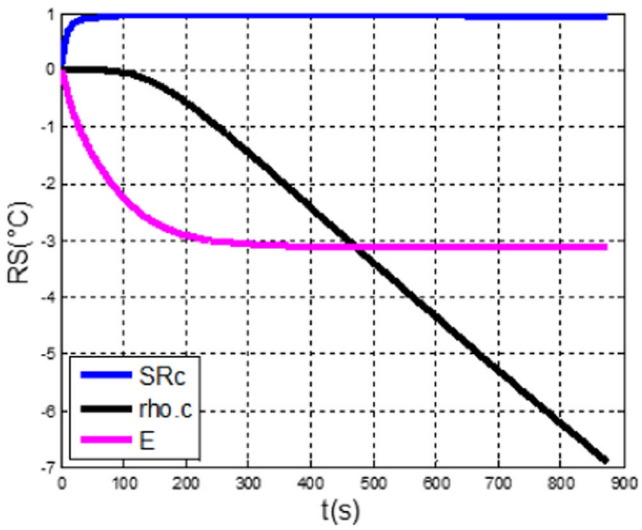
RS(°C)
t(s)
SRc
rho.c
E

b)

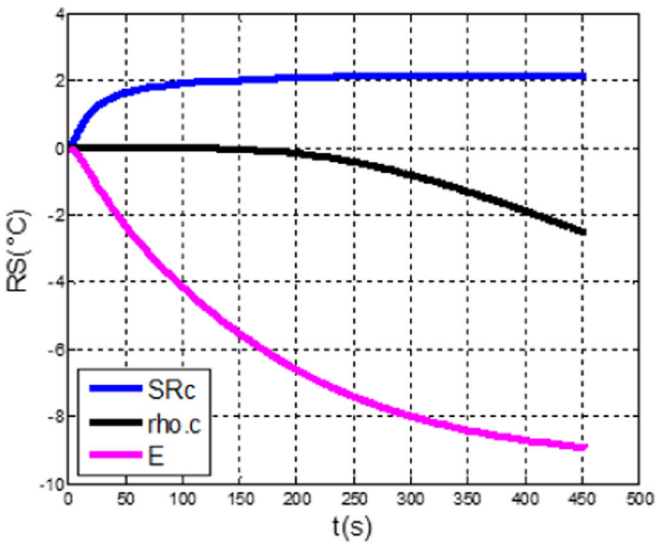
RS(°C)
t(s)
SRc
rho.c
E

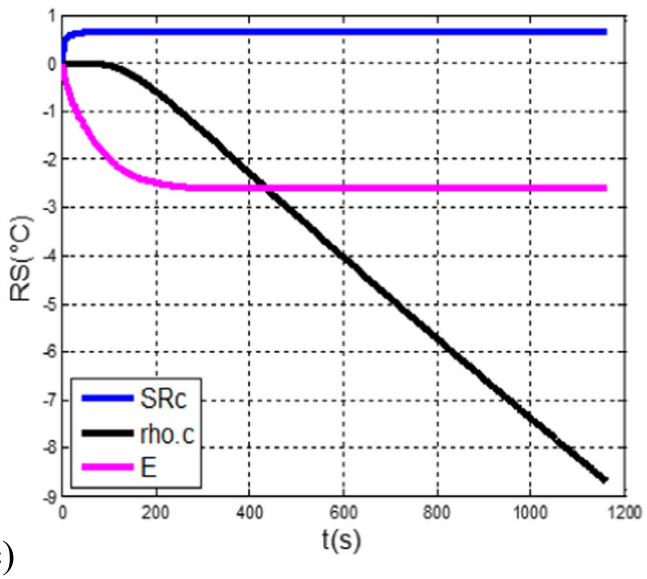
RS(°C)
t(s)
SRc
rho.c
E

c)

– The reduced sensitivities of the temperature to the volumetric heat capacity are correlated with thermal contact resistance at short times, but are uncorrelated with thermal effusivity at long times. A better pre-estimation of volumetric heat capacity can be done from time 300 s.
– The sensitivity of the temperature to the thermal contact resistance with the insulating material is negligible. This can be justified to the extent that its value has been set at 10^{-10} °C W^{-1} [21].

The pre-estimation of the thermophysical parameters in the indicated time intervals would facilitate the convergence of the Levenberg Marquart algorithm for the estimation of E and ρc_p by the complete model. With the pre-estimated values of E and ρc_p, the residue curves observed in Fig. 3a, c or d are perfectly centred.

7 Experimental results and discussion

Figure 3 shows the profiles of the experimental and simulated temperature curves for Iroko in the radial (through de fiber) direction at 7%MC (Fig. 3a) and the same sample with a water content of 32% (Fig. 3b). The two profiles show that the heating process takes more time in wet wood.

Figure 3b presents the residues curve of Iroko at 32% MC and shows that the water content has a significant influence on the thermophysical properties. The residues are not centered at 0 °C, indicating that the quadrupole model developed is no longer valid to estimate thermophysical parameters at this water content for Iroko. For Tali and Bilinga, the residues are centered at 0 °C above 30% MC (Fig. 3c, d). This is due to the density of each material. It can be observed that the developed completed model minimizes the sum of quadratic errors between $T_{exp}(t)$ and $T_{mod}(t)$. For Tali and Bilinga, at high water content, the residues are centered to 0 °C.

From the complete model, an estimation of E and $\rho c_p = (\rho c_p)_{exp}$ was obtained for five values of the water content.

The pre estimated values of thermal effusivity are presented in Table 4. Those values are compared to results given by the complete model. There are in good agreement. The maximum deviation between pre estimated and complete model values is less than 5%.

The calculation of volumetric heat capacity with specific heat obtained by the box method [15] is also presented in Table 4. Comparison with the results obtained by the complete model produces low deviations (0,1%–5%). Another method was to calculate volumetric heat capacity by relation (3). Values for the selected species are presented in Table 5. Results are in good agreement with small deviations.

This validation permitted to deduce the thermal conductivity from the relation (6):

$$\lambda = \frac{E^2}{\rho C_p} \tag{6}$$

The thermal diffusivity is therefore given by relation (7):

$$a = \frac{\lambda}{\rho C_p} \tag{7}$$

Table 4 Thermal effusivity and volumetric heat capacity in transverse direction

	MC (%)	ρ (kg.m^{-3})	E_{simpl} (J m^{-2} K^{-1} s$^{-1/2}$)	E_{comp} (J m^{-2} K^{-1} s$^{-1/2}$)	ρCp_{exp} (J m^{-3} K^{-1})	Cp (J kg^{-1} K^{-1})	ρxCp (J m^{-3} K^{-1})	D E (%)	D ρCp (%)
Bilinga	34,14	863	662,261	695,840	1,92 10^6	2350,17	2,16 10^6	5,07	5,47
	25,00	800	621,529	645,489	1,86 10^6	2235,00	1,79 10^6	3,86	3,95
	18,85	760	519,177	548,483	1,61 10^6	2070,54	1,59 10^6	4,45	0,92
	11,72	715	466,800	474,774	1,30 10^6	1907,00	1,36 10^6	1,71	4,86
	5,00	672	417,258	439,215	1,05 10^6	1650,13	1,19 10^6	5,26	3,59
Tali	35,14	1096	647,000	644,616	2,52 10^6	2209,84	2,42 10^6	0,37	4,01
	28,73	1044	602,025	617,202	2,22 10^6	2081,60	2,17 10^6	2,46	1,99
	16,40	944	527,643	527,102	1,78 10^6	1837,69	1,73 10^6	0,10	2,36
	11,22	902	487,198	485,502	1,58 10^6	1753,00	1,58 10^6	0,35	0,17
	6,66	865	497,536	446,341	1,40 10^6	1630,18	1,41 10^6	0,48	0,89
Iroko	28,00	885	638,097	655,412	1,81 10^6	2100,26	2,09 10^6	2,71	4,17
	18,23	817	592,855	610,187	1,63 10^6	2055,85	1,68 10^6	2,92	3,13
	15,05	795	554,542	570,899	1,51 10^6	1979,83	1,57 10^6	2,95	3,99
	12,01	774	531,819	546,576	1,40 10^6	1907,28	1,48 10^6	2,77	5,17
	5,72	730	407,575	438,137	9,92 10^5	1495,78	1,21 10^6	4,67	4,67

D E relative difference between E_{simpl} and E_{comp}, *DρCp* relative difference between ρCp_{exp} and ρx Cp

Table 5 Experimental and numerical volumetric heat capacity

	MC (%)	ρCp $_{exp}$ (J m^{-3} K^{-1})	ρCp (J m^{-3} K^{-1})	D Cp (%)
Bilinga	34,84	1,92E+06	1,81E+06	5,68
	25,00	1,86E+06	1,77E+06	4,93
	18,85	1,61E+06	1,58E+06	1,91
	11,72	1,30E+06	1,19E+06	8,35
	5,00	1,05E+06	1,01E+06	3,87
Tali	35,14	2,52E+06	2,33E+06	6,57
	28,73	2,22E+06	2,11E+06	4,77
	16,40	1,78E+06	1,69E+06	4,71
	11,22	1,58E+06	1,52E+06	3,94
	6,66	1,40E+06	1,36E+06	2,59
Iroko	28,00	1,81E+06	1,82E+06	0,48
	18,23	1,63E+06	1,54E+06	5,49
	15,05	1,51E+06	1,45E+06	4,34
	12,01	1,40E+06	1,36E+06	3,02
	5,72	9,92E+05	1,08E+06	6,70

The values obtained by the complete model and box method for Tali in the longitudinal direction are observed in Table 6.

The experimental data allows to obtain the thermal conductivity for the moisture content range. Parameters describing the linear fitting curve were given in Fig. 5. The values of regression coefficient R^2 (0,9-0,99), means very good correlations between thermophysical properties and MC. The thermal conductivity of each of the three species has been measured for at least five different water contents varying between 0% and 35%. The evolution of thermal conductivity with water content is presented in Fig. 5a, b, and c in longitudinal, radial and tangential directions respectively. The following observations can be made:

- The thermal conductivities of the wood species considered vary between 0.1 and 0.6Wm^{-1} K^{-1}.
- The RT conductivities are identical for a given species regardless of the water content
- The anisotropy ratio of thermal conductivity is higher for Iroko and Bilinga as compared with Tali.

Table 6 Longitudinal thermal conductivity obtained by the complete model and box method for Tali

MC (%)	λ_{exp} (W/mK)	$\lambda_{box\ method}$ [15] (W/mK)	D (%)	a (m^2/s)
31,68	0,565	0,562	0,56	2,48^{E}-07
25,01	0,530	0,545	2,83	2,80^{E}-07
12,39	0,501	0,492	1,86	3,00^{E}-07
7,73	0,459	0,465	1,38	3,06^{E}-07
5,07	0,441	0,449	1,72	3,31^{E}-07

D relative difference between λ_{exp} and $\lambda_{box\ method}$

The results show that the wood species considered have lower thermal conductivities than other construction materials [21, 25]. Thermal conductivity increases slowly and linearly with the moisture content below the fiber saturation point. The values of thermal conductivity at 30% MC are considerably higher than the values at a moisture content of 5% MC. The variation is not the same for each species. For example, in the longitudinal direction, a 1% increase in water content induces an increase in thermal conductivity by 0.2% for Bilinga, 0.4% for Tali and 0.3% for Iroko approximately. This is probably due to the variability and wood content of each species.

Figure 5 shows that thermal conductivity has similar characteristics in the tangential and radial directions. This is in agreement with many authors who claimed that the values of thermal conductivity in the radial and tangential directions are almost the same. Tali which has the highest density wood present highest values of thermal conductivity in the longitudinal direction. Moreover, when comparing the findings for Iroko and Tali (Fig. 5b and c), it is obvious that longitudinal thermal conductivity of Iroko is lower than that of Tali. The comparison of radial and tangential thermal conductivities shows the opposite result. Thermal conductivity of Iroko is higher than that of Tali. This finding can be attributed to the amount of the different cell types: tracheids, vessels, fibres and parenchyma cells. In particular, it is attributed to the amount of longitudinally oriented tissue versus the amount of radially oriented ray cells [26]. In Iroko wood, the amount of ray cells is higher as compared with Tali. It follows that the amount of longitudinally oriented tissue is lower in Iroko compared to Tali. Consequently, at approximately the same density, longitudinal thermal conductivity of Iroko is comparably lower while radial thermal conductivity is higher than that of Tali wood.

The RT thermal conductivities are approximately two times smaller than in the longitudinal direction for Bilinga and Iroko. For Tali, they are three times smaller. This phenomenon is because the cross walls contribute negligibly to heat transfer in transverse directions. When the heat flows in the RT directions, the cross walls are in series with the air inside the cell lumens and the thermal resistance of the air dominates. However, the thermal conductivity of air is 20 to 30 times smaller than that of the cell walls and thus, the bulk of the heat is conducted along the side walls linking the hot and cold surfaces of the wood [27].

The anisotropy ratio of thermal conductivity is presented in Table 7. There is a small variation with the water content for a given species. This ratio is higher for Iroko and Bilinga.

Based on Fig. 5, the thermal conductivity can be expressed in the form $\lambda = \lambda_{dry}(1 + \alpha X)$. The values of α are given in Table 8. It is observed that the factor α varies within a certain

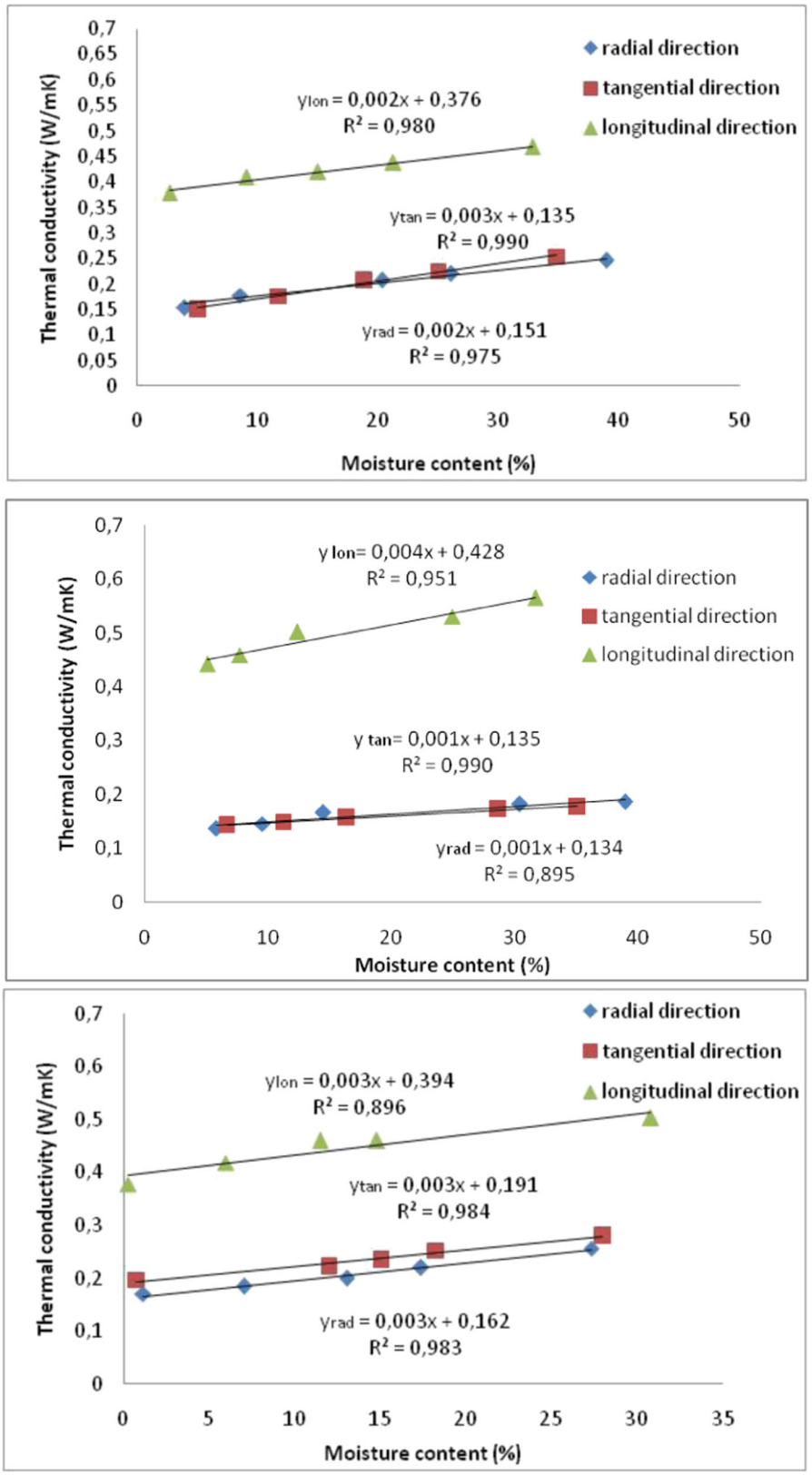

Fig. 5 Thermal conductivity as a function of the water content for selected species: **a** Bilinga, **b** Tali, **c** Iroko

range and is lower for Tali than Iroko and Bilinga. This is partly because of variability in wood structure.

More generally, the three selected species are less conductive materials than usual materials used in construction. Their

Table 7 Anisotropy ratio of thermal conductivity

Moisture content	$\frac{\lambda_{TR}}{\lambda_L}$		
	10%	20%	30%
Bilinga	0,441	0,459	0,453
Tali	0,307	0,303	0,299
Iroko	0,473	0,480	0,492

thermal conductivities are less than 0.8 Wm^{-1} K^{-1} in all the directions. In a building, sawn lumber in the longitudinal direction can be used as supporting elements because its mechanical properties are better, while timber in radial and tangential directions can serve as filling elements. Tali among the three species yields the best results if a combination of resistance and comfort is considered.

The variation of thermal diffusivity in LRT directions with MC is represented in Fig. 6. Diffusivity decreases significantly and almost linearly as water content increases for all species.

It can be observed in Figs. 5, and 6 that the thermal conductivity and diffusivity for three woods is close to each other for the radial and tangential directions. At 20% of MC for example, the thermal conductivity is closer for Bilinga and Tali. Those two species are high density woods with small holes while Iroko is a medium density wood with high amount of ray cells. The ratio of tangential to radial conductivity is primarily determined by the volume of ray cells in hardwoods. Geometric differences in the two directions had little effect on the diffusivity [28].

Figure 7 presents the evolution of volumetric heat capacity as a function of the moisture content. The increase in volume heat capacity of selected wood species with increasing moisture content is observed and can be explained by the highly different heat capacities of wood particles and water. It is known that the heat capacity of water is considerably higher than that of wood. Therefore, increase in the quantity of water in the structure of wood causes an increase in heat capacity of the wood. Wood, being a porous biomaterial, contains small holes that greatly influence the mechanism of heat transfer, and also the heat capacity. In timber moistening, when air is replaced with water, specific heat of timber is increased. The heat capacity of wood depends on the temperature and moisture content. On the other hand, the chemical composition only varies slightly between different species. That is why variations between wood species are very small.

8 Conclusion

This paper presents the experimental measurements of thermal properties of tropical woods. The asymmetrical hot plate method was used to characterize the thermal behavior of three tropical wood species. The influence of the water content and the direction of fibers on thermophysical properties was investigated. Linear relations were obtained in the data range of moisture content. An increase in thermal conductivity and volumetric heat capacity of tropical wood due to an increase in moisture content was observed. Iroko, which has the lowest density, presents the higher variation of conductivity when fibers are parallel to the direction of the heat flow. Tali, which has the highest density, has the lowest values of conductivity in the radial and tangential directions. Approximately 1% increase in water content induces a 0,2% increase in conductivity in the longitudinal direction for Bilinga, 0.4% for Tali and 0,3% for Iroko. The influence of anisotropy is clearly established. Thermal conductivity is 2–3 times greater in the longitudinal direction than in the radial and tangential directions. The thermal conductivity of selected species varied between 0,15 and 0,30 Wm^{-1} K^{-1} in the radial and tangential

Table 8 factor α as a function of transversal thermal conductivity

λ_{dry} (Wm^{-1} K^{-1})	Moisture content (%)	λ (W m^{-1} K^{-1})	α
Bilinga	34,84	0,252	0,025
$\lambda_{dry=0,151}$ W m^{-1} K^{-1}	25,00	0,224	0,026
	18,85	0,206	0,028
	11,71	0,175	0,025
Tali	35,14	0,176	0,009
$\lambda_{dry=0,134}$ W m^{-1} K^{-1}	28,72	0,172	0,010
	16,39	0,156	0,010
	11,22	0,149	0,009
Iroko $\lambda_{dry=0,162}$ W m^{-1} K^{-1}	28,00	0,280	0,017
	18,23	0,252	0,017
	15,05	0,235	0,016
	12,01	0,223	0,014

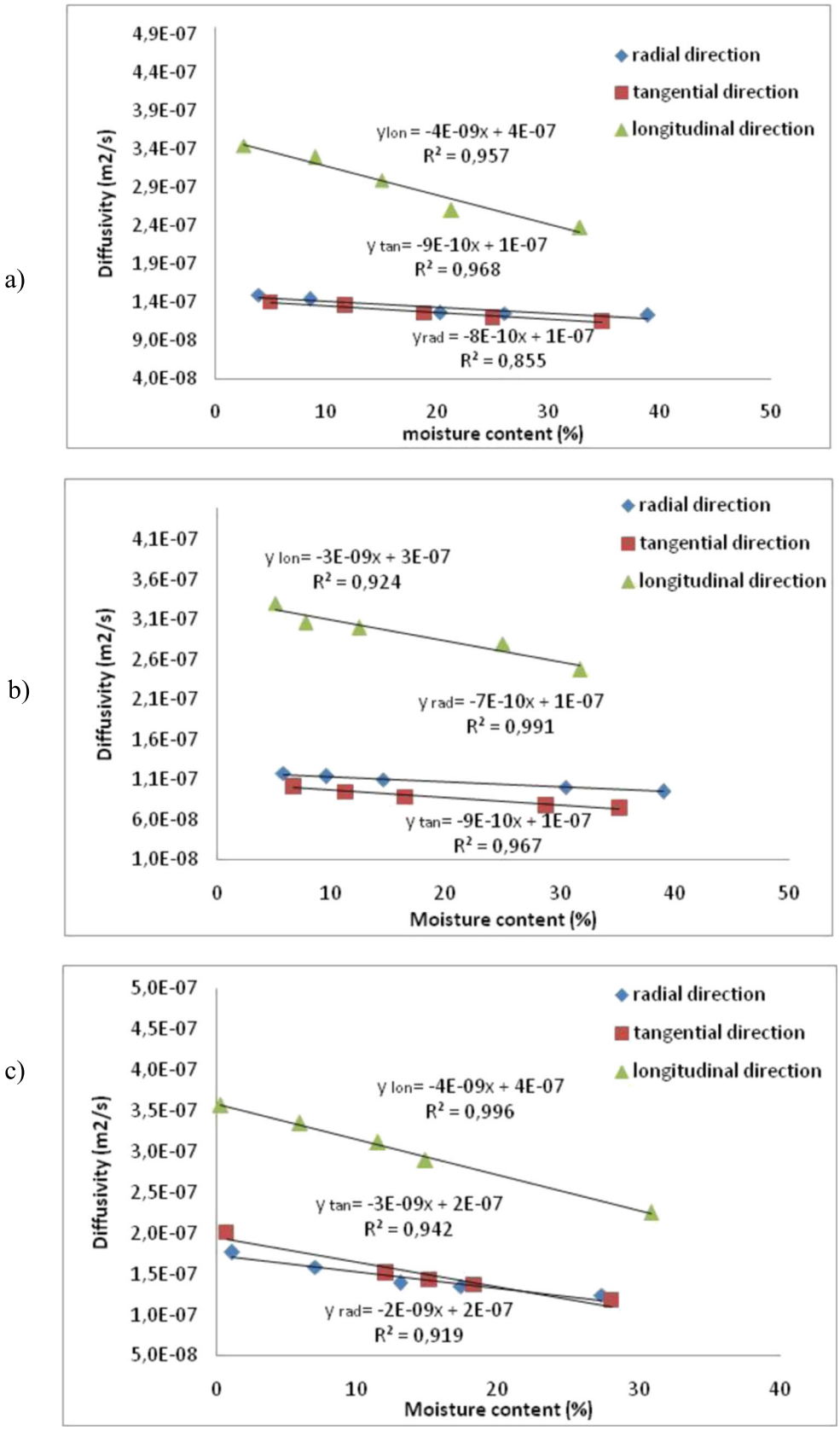

Fig. 6 Thermal diffusivity as a function of the water content for selected species: **a** Bilinga, **b** Tali, **c** Iroko

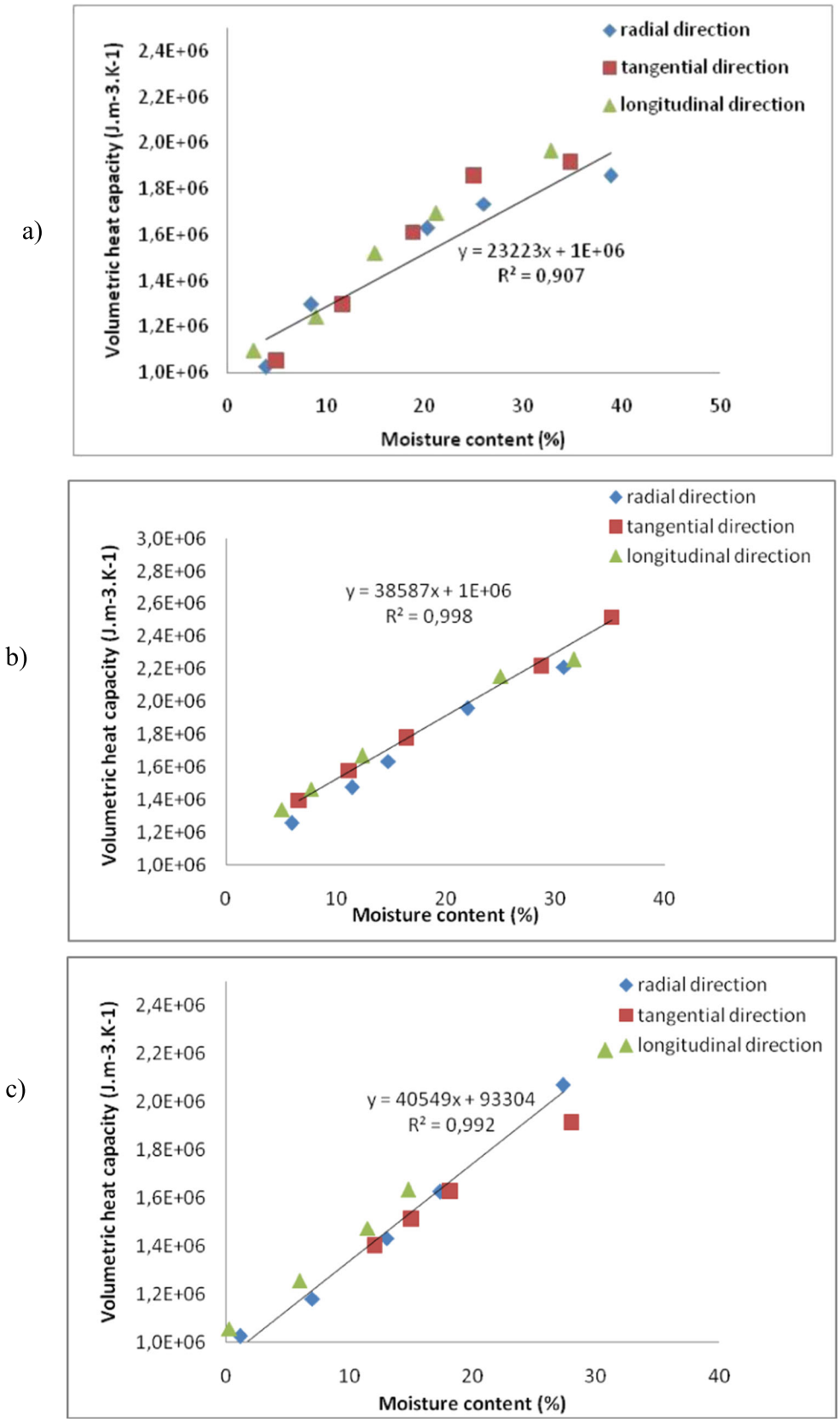

Fig. 7 Volumetric heat capacity as a function of the water content for selected species: **a** Bilinga, **b** Tali, **c** Iroko

directions. Diffusivity is negatively correlated to moisture content. Volumetric heat capacity is not really influenced by the direction of the heat flow. Below the saturation of the fibers, the thermal conductivity of all the selected species is less than 0,8 Wm^{-1} K^{-1}. Consequently, the wood species studied can be considered as good insulating materials. These species can therefore easily replace the common materials such as agglomerates or earthenware bricks which will contribute for a better thermal comfort. The knowledge of the equilibrium water content of the wood studied can help to optimize the energy design of buildings.

References

1. Lau LC, Lee KT, Mohamed AR (2012) Global warming mitigation and renewable energy policy development from the Kyoto protocol to the Copenhagen accord - a comment. Renew Sust Energ Rev 16(7):5280–5284
2. Pérez-Lombard L, Ortiz J, Pout C (2008) A review on buildings energy consumption information. Energy and Buildings 40(3):394–398
3. Gustavsson L, Joelsson A, Sathre R (2010) Life cycle primary energy use and carbon emission of an eight-storey wood-framed apartment building. Energy and Buildings 42(2):230–242
4. ADEME, Rapport Type 2011, Audit-Energétique-Bâtiment. www.ademe.fr
5. Malsot J, Deroubaix G, Paquet Ph, Raji S, Prieur A, Lochu S (2005) Extention de l'égibilité de la séquestration forestière du carbone à l'ensemble des stocks de la filière bois. VIIIème Colloque ARBORA, Carbone, Foret, Bois. ISTAB
6. Elimbi A et al (2005) Protocole d'analyses des matières premières et produits finis au laboratoire, MIPROMALO
7. Steinhagen HP (1977) Thermal conductive properties of wood, green or dry, from −40 to +100°C: a literature review, USDA Forest Service general technical report (FPL-9), Wisconsin
8. Suleiman BM, Larfeldt J, Leckner B, Gustavsson M (1999) Thermal conductivity and diffusivity of wood. Wood Sci Technol 33:465–473
9. Jia D, Afzal MT, Gongc M, Bedane AH (2010) Modeling of moisture diffusion and heat transfer during softening in wood densification. Int J Eng 4:191–200
10. Siau JF (1995) Wood: influence of moisture on physical properties. Virginia Polytechnic Institute and State University, Blacksburg
11. Harada T, Hata T, Ishihara S (1998) Thermal constants of wood during the heating process measured with the laser flash method. J Wood Sci 44:425–431
12. Kol HS (2009) The transverse thermal conductivity coefficients of some hardwood species grown in Turkey. For Prod J 59:58–63
13. Sonderegger W, Hering S, Niemz P (2011) Thermal behaviour of Norway spruce and European beech in and between theprincipal anatomical directions. Holzforschung 65:369–375
14. Rohsenow W, Hartnett J, Ganic E (1973) Handbook of heat transfer fundamentals. McGraw-Hill Book Company, New York
15. Ngohe-Ekam PS, Meukam P, Menguy G, Girard P (2006) Thermophysical characterization of tropical wood used as building materials: with respect to the basal density. Constr Build Mater 20:929–938
16. Cherki A, Remy B, Khabbazi A, Jannot Y, Baillis D (2014) Experimental thermal properties characterization of insulating cork-gypsum composite. Constr Build Mater 54:202–209
17. Bal H, Jannot Y, Quenette N, Chenu A, Gaye S (2012) Water content dependence of the porosity and thermal capacity of laterite based bricks with millet waste additive. Constr Build Mater 31:144–150
18. Laaroussi N, Lauriat G, Garoum M, Cherki A, Jannot Y (2014) Measurement of thermal properties of brick materials based on clay mixtures. Constr Build Mater 70:351–361
19. Mvondo RRN, Meukam P, Jeong J, De Sousa Meneses D, Nkeng EG (2017) Influence of water content on the mechanical and chemical properties of tropical wood species. Results in Physics 7:2096–2103
20. Gerard J, Kouassi AE, Daigremont C, Detienne P, Fouquet D, Vernay M (1998) Synthèse sur les caractéristiques technologiques de référence des principaux bois commerciaux africains. Serie FORAFRI No. Document 11. CIRAD-Foret, Montpellier 187p
21. Damfeu JC, Meukam P, Jannot Y, Wati E (2017) Modeling and experimental determination of thermal properties of local wet buildings materials. Energy and Buildings 135:109–118
22. MacLean JD (1941) Thermal conductivity of wood. Heat Piping Air Cond 13:380–391
23. Jannot Y, Remy B, Degiovanni A (2009) Measurement of thermal conductivity and thermal resistance with a tiny hot plate high temp. High Pressure 39:11–31
24. Jannot Y, Zoubir A, Kanmogne A (2006) Transient hot plate method with two temperature measurements for thermal characterization of metals. Meas Sci Technol 17:69–74
25. Meukam P, Jannot Y, Noumowe A, Kofane TC (2004) Thermophysical characteristics of economical building materials. Constr Build Mater 18:437–443
26. Vay O, De Borst K, Hansmann C, Teischinger A, Müller U (2014) Thermal conductivity of wood at angles to the principal anatomical directions. Wood Sci Technol 49:577–589
27. Couturier MF, George K, Schneider MH (1996) Thermo-physical properties of wood-polymer composites. Wood Sci Technol 30:179–196
28. Ugolev BN (2001) Wood science with fundamentals of forest merchandizing. Publishing house of MGUL, Moscow 340 p